Depik Jurnal Ilmu-Ilmu Perairan, Pesisir dan Perikanan (2025), Special Issue The 5th ICFM: 75-86

DEPIK
Jurnal Ilmu-Ilmu Perairan, Pesisir dan Perikanan
Journal homepage: www.jurnal.usk.ac.id/depik

Mapping and validation of spatial algorithm for monitoring turbidity of seagrass habitat using sentinel-2B imagery in Ternate Island

Rustam Effendi Paembonan [1,2,*], Dietriech Geoffrey Bengen [3], I Wayan Nurjaya [3], Syamsul Bahri Agus[3], Nyoman Metta N Natih [3], Beginer Subhan [3], Joko Santoso [4]

[1] *Graduate Student of Doctoral Programme, Department of Marine Science and Technology, Faculty of Fisheries and Marine Science, IPB University. Jl Agatis, Bogor, 16680, West Java, Indonesia*
[2] *Marine Science Department, Faculty of Fisheries and Marine Science, Khairun University. Gambesi Campus, Ternate 97716, North Maluku, Indonesia*
[3] *Department of Marine Science and Technology, Faculty of Fisheries and Marine Science, IPB University. Jl Agatis, Bogor, 16680, West Java, Indonesia*
[4] *Department of Aquatic Products Technology, Faculty of Fisheries and Marine Science, IPB University. Jl Agatis, Bogor, 16680, West Java, Indonesia*

ARTICLE INFO

Keywords:
remote sensing
ecosystems
coastal
sedimentation
North Maluku

DOI: 10.13170/depik.0.0.46989

ABSTRACT

Turbidity is a parameter of the marine environment that greatly affects the condition of seagrass whose habitat is an intertidal zone in shallow sea waters. Seagrass is an important type of ecosystem that can be found in several coastal areas of Ternate Island. This study aims to analyze the turbidity conditions of seagrass habitat waters and apply a remote sensing algorithm using Sentinel 2B images. The turbidity research method was carried out by field measurements. The turbidity algorithm model used refers to references with mathematical equations (Rrs665-0.014)/0.013, and the development of a new algorithm as a comparison algorithm. Both algorithms were validated with field data to determine the level of accuracy using the Normalized Mean Absolute Error (NMAE) and determination coefficient (R^2). The results were obtained from turbidity data with values ranging from 0.3 NTU to 1.5 NTU with an average value of 0.87 ± 0.45 NTU. The Sentinel 2B image in this study was restored with geometric corrections, atmosphere, radiometric digital values, land masking, and sun glint. The turbidity algorithm model used obtained good accuracy in mapping and monitoring the turbidity of seagrass habitat waters on Ternate Island. The application of the turbidity algorithm used as a reference in this study has an NMAE value of 50.44 and R^2 of 0.8822, while the newly discovered turbidity algorithm has an NMAE value of 29.38 and R^2 of 0.8827.

Introduction

Seagrass is a type of vegetation in shallow waters that can be found as seagrass beds in coastal areas and small islands (Dewi *et al.,* 2017). Seagrass ecosystems have positive roles and benefits by helping the sustainability of other biological communities within and outside these ecosystems (Duarte *et al.,* 2013). Seagrass is known as an important marine ecosystem that serves as a habitat for various marine organisms in shallow waters (Sari *et al.,* 2021). Seagrass plays an important role in supporting nutrient cycling and carbon dioxide sequestration, thus maintaining ecological balance in coastal areas (Dewi *et al.,* 2021). Seagrass can improve water quality and mitigate erosion because it can dampen waves to reduce sedimentation (Chisholm, 2009; Ondiviela *et al.*, 2014).

Seagrass ecosystems are highly susceptible to marine environments with turbid water quality (Lessy and Ramili, 2018). Turbidity is an indication of the amount of suspended particles present in the water column (Davies-Colley & Smith, 2007). Marine waters that have high turbidity levels are inversely proportional to the level of brightness (Al Tanto *et al.,* 2018). Increased turbidity of waters can affect light penetration, inhibiting photosynthesis and seagrass growth, making these ecosystems vulnerable to environmental threats (Jo *et al.,* 2023). Sources of water turbidity can be caused by natural factors and human activities. Turbidity factors in marine waters

* Corresponding author.
Email address: effendirustam400@gmail.com

p-ISSN 2089-7790; e-ISSN 2502-6194
Received 1 April 2025; Received in revised 1 May 2025; Accepted 15 July 2025
Available online 30 July 2025

can be caused by mountain eruptions, whose material is carried by water through rivers so that it reaches the coast. Turbidity around the coast can also be caused by unstable coastal substrates influenced by wave interactions. Turbidity factors are caused by human activities such as mining, coastal development, and waste disposal. The potential for increased turbidity that may reduce the health of seagrass ecosystems on Ternate Island is very large because the island is an active volcanic island and there are many activities because it is inhabited by a population of 196.130 people (Najamuddin *et al.,* 2024). The island is classified as a small island with a land area of 10.099.88 ha as stated in the RTRW document of Ternate City 2010-2030 (Paembonan *et al.,* 2022). High seawater turbidity can disrupt the ecological balance of the waters because it reduces light penetration needed by seagrasses for photosynthesis (Sarinawaty *et al.,* 2020). Therefore, monitoring turbidity is essential to maintain the sustainability and protection of seagrass ecosystems (Supriyadi *et al.,* 2018).

Water turbidity data in seagrass habitats that are difficult to reach directly can be mapped using remote sensing technology through the use of satellite imagery. One of the satellites that has high spatial resolution and is able to detect turbidity variations in shallow water habitats is Sentinel-2 B. The success of remote sensing technology through the use of Sentinel-2 imagery in extracting information on the distribution of suspended solids in the water column found high concentrations in areas near land and decreasing towards the open sea (Ajiperwata *et al.,* 2023). The utilisation of satellite imagery data enables more accurate identification of coastal objects, including seagrass ecosystems, to support sustainable monitoring (Cahyaningsih & Hartono, 2018).

The accuracy of water turbidity mapping in seagrass ecosystems can be improved with the use of customised algorithms validated with in situ data. Previous studies have shown that spatial algorithms tailored to the local environment can provide more accurate turbidity measurements than generalised algorithms (Xu *et al.,* 2023). An algorithm for turbidity estimation using Sentinel 2A data in the Kneiss Islands of Gabes Bay, Tunisia, has successfully obtained spatial turbidity data with a fairly good coefficient of determination (Katlane *et al.,* 2020). In addition, spatial algorithms of remote sensing satellite image data can be used for planning and development in various coastal areas in Indonesia (Wicaksono *et al.,* 2019). Ternate Island as a small volcanic island and bearing various human activities, and the utilisation of sentinel image data is needed to obtain spatial information on the turbidity of coastal waters, especially those with seagrass ecosystems.

Materials and methods

Location and time research

This research was conducted in Ternate Island, North Maluku Province, in September 2024 (Figure 1). Sampling of water turbidity data was carried out around beaches that have seagrass beds, with a total of 12 sampling points. Tools and materials used in data collection include one unit of Garmin GPS with an accuracy level of 3 metres that serves to take coordinate points, one unit of Horiba U-51 Series Multi-Parameter Water Quality Meter to measure water turbidity, one unit of cannon camera for documentation and one sheet of location map containing thematic seagrass distribution around Ternate Island. The field data that has been collected is then tabulated for further analysis.

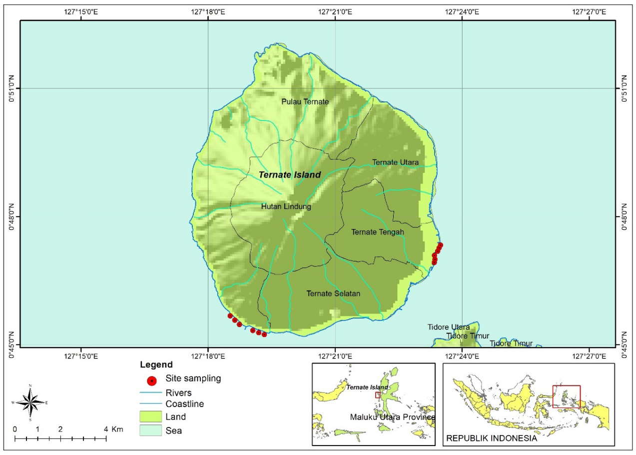

Figure 1. Study the site map of Ternate Island, North Maluku, Indonesia

Collection, processing and restoration of Sentinel 2 B Imagery

Sentinel 2B image data was downloaded from the website https://scihub.copernicus.eu. The sentinel image recording coverage used in this study uses a cloud cover of 0 - 30%. The research location, which includes Ternate Island, especially coastal areas that have seagrass beds, must be free from the influence of clouds. Image data processing and recovery using SNAP 11.00, QGIS 3.32, and other digital image data processing software. Image data processing and restoration include geometric correction, area cropping, atmospheric correction, radiometric correction, land masking, and sun glint correction.

Algorithm selection of aquatic turbidity

The type of algorithm for turbidity mapping chosen in this study is the algorithm developed by Katlane *et al.,* 2020. This algorithm was developed from Sentinel 2 image data using a bandwidth of λ=665 nm, a spatial resolution of 10 and a regression coefficient value (R^2) of 0.70.

Development of a new algorithm for aquatic turbidity

This research developed a new algorithm to map the distribution of turbidity around the Terate Island sea. The type of algorithm developed from Sentinel 2B image with central wavelength (nm), namely band 2-blue λ = 492.1 nm, band 3-green λ = 559.0 nm, band 4-red 664.9 nm and band 8-NIR λ = 832.9 nm with a spatial resolution of 10 m each. The development of the new algorithm uses multiple regression analysis with the y-variable expressed by in situ data and the x-variables expressed by each of the Sentinel 2B image bands used in this study.

Data analysis

Data analysis in this study was carried out based on several mathematical equations:

1. Geometric, atmospheric, and radiometric digital value correction of Sentinel 2B imagery. Geometric and atmospheric corrections were performed automatically using SNAP 11.00 and QGIS 3.32 software. Radiometric correction of the digital values of Sentinel 2B imagery was performed on each band based on the offset value on the x-axis of the image histogram before correction (Mather, 2004) using the equation:
$$DN'_i = DN_i - offset_{band\ i}$$
where DN'i : Digital value of band i image after correction (nm), DN_i : digital value of band I image after correction, and $offset_{bandi}$: radiometric calibration factor (nm) of each band i.
2. Sun Glint Correction (Hedley *et al.,* 2005) with the equation:
$$R'_i = R_i - b_i\ (R_{NIR} - Min_{NIR})$$
where R'_i is the corrected pixel value, R_i is the initial value of the pixel value, bi is the slope of the regression line, R_{NIR} and is the minimum value among the Min_{NIR} of the pixel samples. Sunglint correction process using the Empirical Line of Sight Correction (ELOS) method.
3. Turbidity algorithm of Katlane *et al.,* 2020 with equation:
$$TU = \frac{(Rrs665 - 0.014)}{0.013}$$
Where TU: digital value of clarity and Rrs665: band red
4. Multiple linear regression equation (Rahmad *et al.,* 2019) to construct a new algorithm with the equation:
$$Y = b_o + b_1X_1 + b_2X_2 + \cdots + b_nX_n + \varepsilon_i$$
Where y: new turbidity algorithm which is the dependent variable, X_1, X_2, X_3, X_n: Sentinel 2B image bands which are independent variables, b_o,b_1,b_2,b_3: regression parameters whose values are unknown, ε_i: error value.
5. The algorithm accuracy test is validated using Normalised Mean Absolute Error (NMAE) and the coefficient of determination (R2). NMAE is calculated with the equation:
$$\text{NMAE (\%)} = \left(\frac{\sum_{i=1}^{n}|y_i - y'_i|}{n\ x\ Mean(y)}\right)\ x\ 100\%$$
Where: y_i: Actual value for 1th data, y'_i: Predicted value for the 1th data, n: Number of data. NMAE has a value of 0 to 1 (can also be expressed in per cent), the lower the NMA value indicates the more accurate the model.

The coefficient of determination (R^2) is calculated by the equation:
$$R^2 = \left(\frac{N\sum_{xy}(\sum_x(\sum_y)}{\sqrt{N(\sum x^2 - (\sum x)^2}\sqrt{N(\sum x^2) - (\sum y)^2}}\right)^2;$$
Where the R^2 value ranges from 0 - 1. The higher the R^2 value, the better the model.

Results

Water turbidity condition in seagrass habitat of Ternate Island

Turbidity measurement results of seagrass habitat waters of Ternate Island sampled at 12 locations ranged from 0.3 NTU to 1.5 NTU with an average value of 0.87±0.45 NTU (Figure 2). The turbidity value of the research site waters in the southern part of Ternate Island which includes K, K2, K3. J1, J2 and J3 are relatively higher than the turbidity values in the eastern waters which include P1, P2, P3, N1, N2, and N3. Variations in turbidity values based on sampling points found insignificant differences in values. The highest value is at sampling point K1 with a value of 1.5 NTU. Turbidity with a value of 1.4 NTU was found at different sampling points K2 and K3. Turbidity values at sampling points J1, J2 and J3 were found to be 1.1 NTU, 0.9 NTU and 1.2 NTU respectively. Water turbidity with a value of 0.7 NTU was found at two sampling points P2 and P3. At sampling point N1, turbidity with a value of 0.6 NTU was found.

The lowest turbidity value was found at three sampling points namely P1, N2 and N3 with a value of 0.3 NTU.

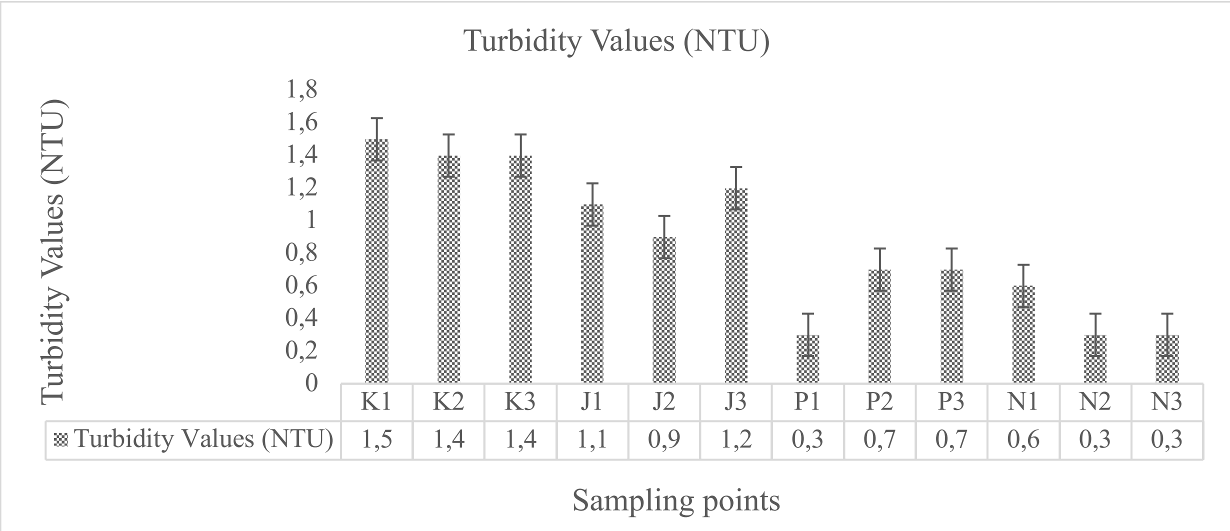

Figure 2. Graph of water turbidity measurement results in seagrass habitat in Ternate Island

Sentinel 2B band characteristics and selection

Sentinel-2B was developed and operated by the European Space Agency (ESA) and launched on 7 March 2017. The satellite was produced to support services and applications such as agricultural monitoring, emergency management, land cover classification and water quality. The Sentinel 2B satellite is an earth observation satellite that acquires high spatial resolution optical imagery with a recording area covering land and coastal waters. This satellite orbits at an altitude of 786 km with a sweep width of 290 km and operates with a coverage area between latitudes 56° south and 84° north. The Sentinel 2B satellite has a temporal time of 5 days. The Sentinel-2B sensor consists of 13 bands with spatial resolutions including 10 metres for four visible and near infrared, 20 metres for six red edge and shortwave infrared bands, and 60 metres for three atmospheric correction bands (Table 1) (https://scihub.copernicus.eu.).

Table1. Sentinel 2B Satellite image band characteristics (Source: https://scihub.copernicus.eu.)

Sentinel-2B bands	Central wavelength (nm)	Bandwidth (nm)	Spatial resolution (m)
Band 1 – Coastal aerosol	442.2	21	60
Band 2 – Blue	492.1	66	10
Band 3 – Green	559	36	10
Band 4 – Red	664.9	31	10
Band 5 – Vegetation red edge	703.8	16	20
Band 6 – Vegetation red edge	739.1	15	20
Band 7 – Vegetation red edge	779.7	20	20
Band 8 – NIR	832.9	106	10
Band 8A – Narrow NIR	864	22	20
Band 9 – Water vapour	943.2	21	60
Band 10 – SWIR – Cirrus	1376.9	30	60
Band 11 – SWIR	1610.4	94	20
Band 12 – SWIR	2185.7	185	20

The Sentinel 2B image data used in this study was recorded on 26 September with the file name S2B_MSIL2A_20240926T015359_N0511_R117_T 52NCF_ 20240926T034203.SAFE. The selection of Sentinel 2B image bands based on Table 1 used in this study totalled 4 bands sourced from the visible and infrared band spectra. The names of the four bands involved include Band 2 - Blue, Band 3 -

Green, Band 4 - Red and Band 8 - NIR with the same spatial resolution of 10 m.

Sentinel 2B Image Processing and Recovery

Atmospheric and geometric corrections were carried out using the Sen2Cor Processor plugin in the SNAP software. SNAP Software performs image correction based on image meta data files that can function automatically in performing atmospheric correction and correction of digital geometric values. Geometric correction on the image uses UTM Zone 52 North projection, World Geodetic System Datum 1984. This corrected image was then resized to cover the area of Ternate Island and its surrounding marine waters.

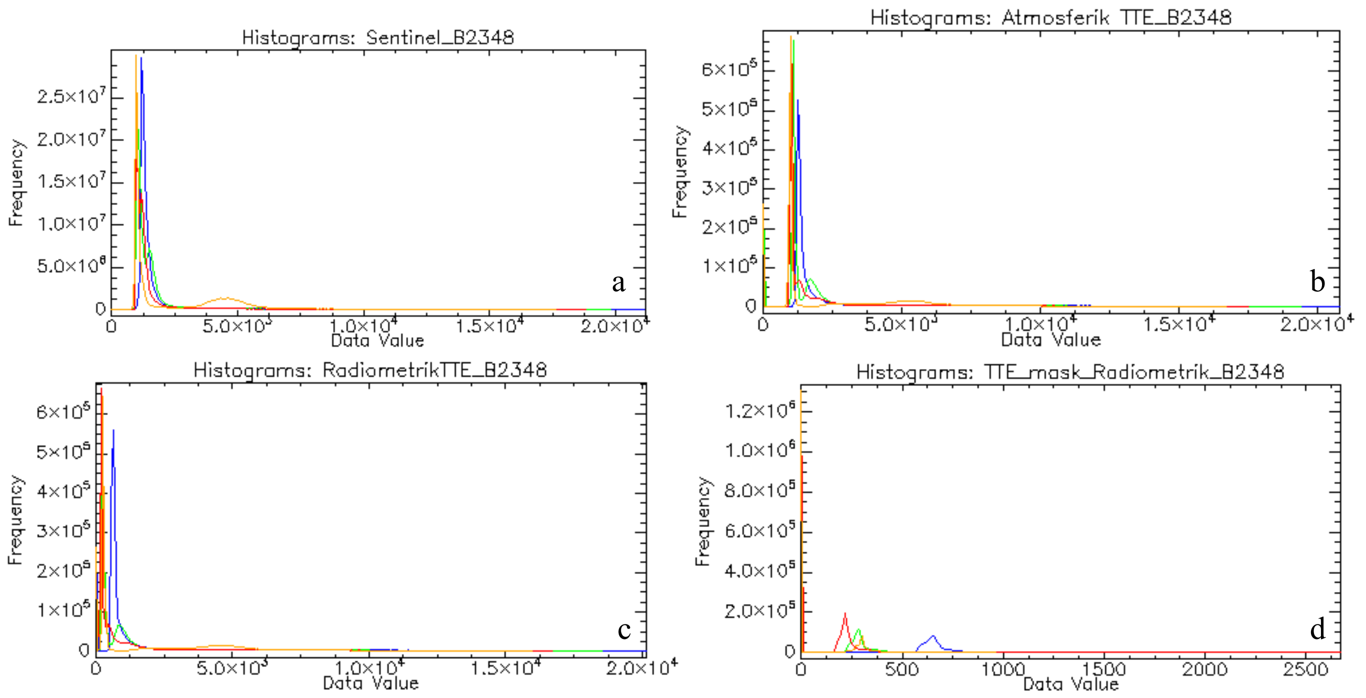

Figure 3. Histograms of atmospheric correction results and radiometric digital values Band 2-blue, 3-green, 4-red and 8 Sentinel B2 images of the research area coverage a. full scene. b. atmospheric corrected image, c. radiometric digital value corrected image, d. land masking result image.

The new image of the research area is atmospherically corrected and the radiometric digital value can be known based on the digital values of the image contained in each histogram (Figure 3). The correction of the radiometric digital value of the image is carried out with the Dark Substrate Correction method, which is the correction of the digital value of the image based on the offset of the digital value contained in the X-axis (Mather, 2004; Paembonan, *et al.*, 2018). The new radiometric digital value corrected image is an image sourced from geometric and atmospheric corrected images (Table 2).

Table 2. Correction radiometric digital values of Sentinel 2B imagery based on research location in Ternate Island

Band Name	Wavelengths (µm)	Atmospheric Digital Values (nm)	Offset Corection Dark Substrat (nm)	Radiometric Digital Values (nm)
Band 2-Blue	0.443	0 - 20828	656	0 – 20172
Band 3-Green	0.560	0 - 19404	847	0 – 18557
Band 4-Red	0.665	0 - 17526	828	0 – 16698
Band 8-NIR	0.842	0 - 16698	726	0 – 15972

Land masking in this study needs to be done to separate land and marine objects (Mikelsons *et al.*, 2021). The separation of these two objects is very important because the radiance value used in the classification process of objects in the water column is not influenced by the radiance value of land, so land-masking is necessary. This step is done by creating a binary image (pixel values 0 and 1) based on the pixel values in band-4 (near infrared) or performing a separation by determining the digital mean value between and water column expressed by pixel value 0 and the land boundary expressed by pixel value 1. The separation of water column and land boundaries in this study uses the Raster Colour Slices method where the digital value of the water column ranges from 0- 695 nm which is expressed by a binary image with a pixel value of 0 and the digital value of the land ranges from 566 - 15972 nm which is expressed by a binary image with a pixel value of 1. To separate land objects with land masking techniques from images B2, B3, B4 and B8 is done by using build masking based on binary images.

Image quality can also be affected by reflected sunlight on the water surface and can reduce image accuracy. Image correction in these conditions is known as sun glint correction and is essential to remove the effects of sun glint from water surfaces. The sun glint correction value is obtained from the slope value of the regression equation obtained from digitising each visible band with the infrared band (Hedley *et al.,* 2005). Sentinel 2B imagery can use Bands 2, 3 and 4 regressed with band 8 (Figure 4).

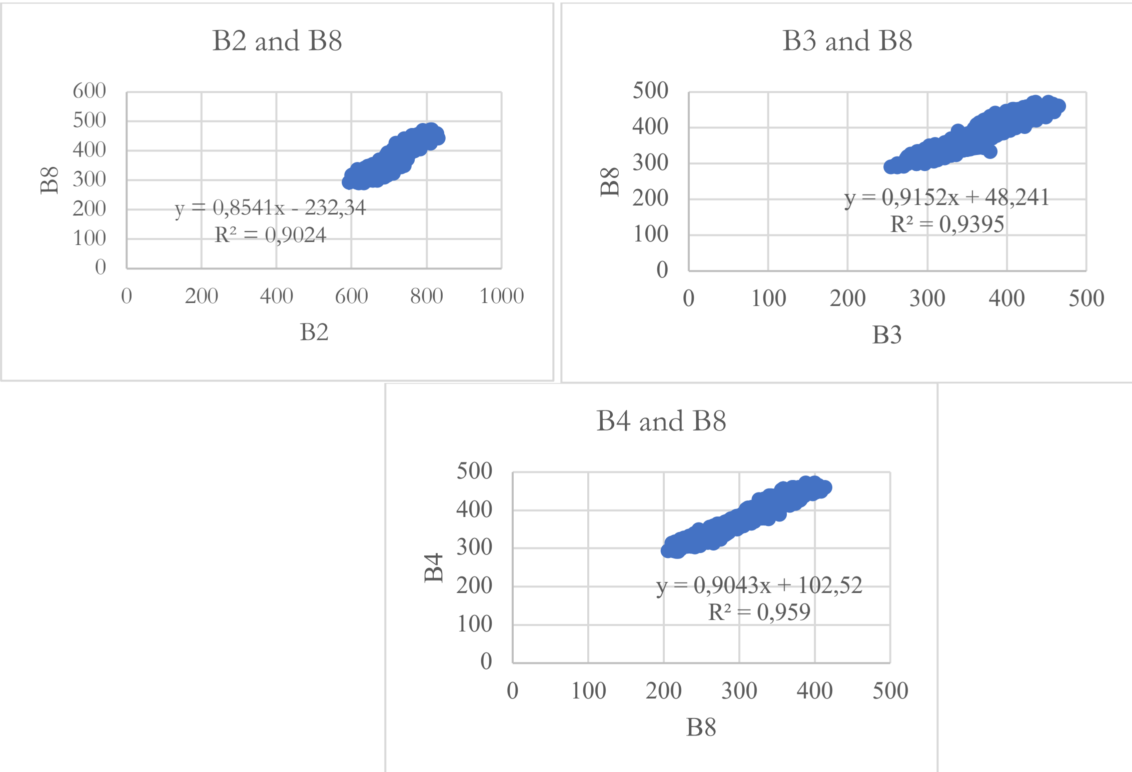

Figure 4. Sun glint correction equation from the regression result graph of bands 2, 3 and 4 with band 8.

Application of Katlane *et al.,* (2020) algorithm for aquatic turbidity mapping

A multispectral image algorithm model that has been used for water turbidity mapping is the algorithm developed by Katlane *et al.,* (2020). This algorithm uses the Sentinel 2A satellite band red with a spectral length of 665 nm. The application of the turbidity mapping algorithm is done by correlating the 665 nm spectral length with in situ turbidity measurements through a regression equation. Quantification of the turbidity algorithm conducted by Katlane *et al.,* (2020) using Sentinel 2A data successfully showed turbidity values that were close to the measured values at sea.

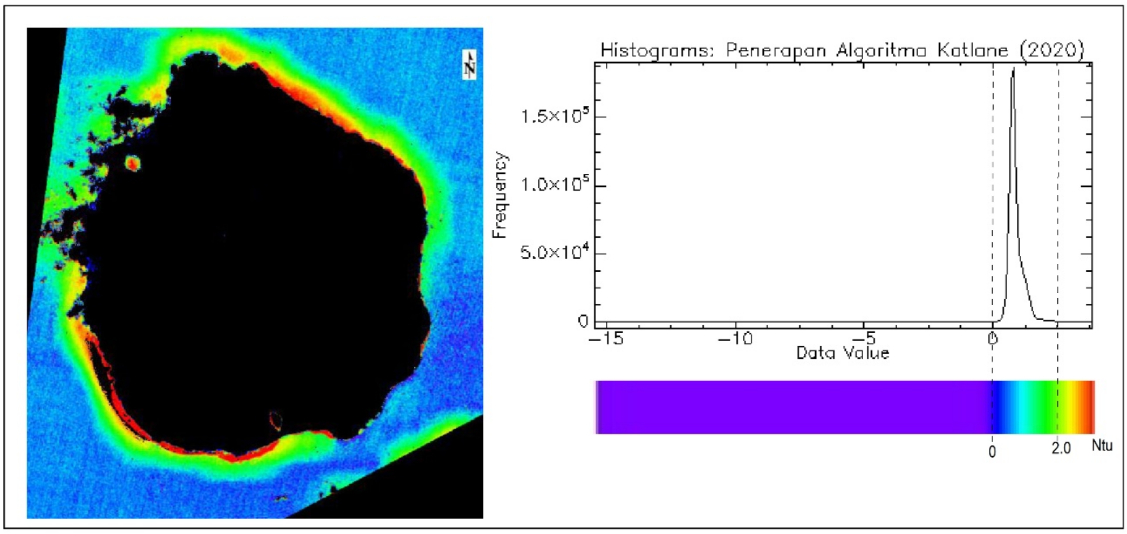

Figure 5. Application of Katlane *et al.,* (2020) Algorithm for mapping turbidity of Ternate Island waters

The application of the Katlane *et al.,* (2020) algorithm to map turbidity distribution on Ternate Island using Sentinel 2B is systematically based on the equation that has been applied to the mapping of water turbidity in the Kneiss Islands in the Gulf of Gabes. The results of turbidity distribution mapping found turbidity values around the coast that were not significantly different from the in situ measurement data (Figure 5). The coefficient of determination (R^2) resulting from the application of the algorithm in this study to the in situ data is 0.8822.

Development of a New Algorithm for Turbidity Mapping and Monitoring

This research developed an algorithm as a comparison algorithm for mapping and monitoring the turbidity of seagrass habitat in Ternate Island using Sentinel 2B imagery. The selected multispectral bands include visible and NIR spectral which include Band 2-Blue, Band 3-Green, Band 4-Red and Band 8-NIR. Algorithm development was performed using linear multiple regression analysis between the spectral value channel as the independent variable (x) and the in situ turbidity measurement results as the dependent variable (y). The results of the analysis found Regression Statistics values for each spectral channel used (Table 3).

Table 3. Multiple liner regression test results between spectral values and in situ data.

Regression Statistics	Intercept	Band 2-Blue	Band 3-Green	Band 4-Red	Band 8-NIR
Standard Error	0.7069	0.000916	0.000679	0.00165	0.000502
t Stat	0.084766	-1.70274	-0.34449	4.747743	0.983777
P-value	0.934821	0.132401	0.740599	0.002089	0.357998
R Square			0.970173		

The results of the multiple liner regression test of spectral values with in situ data based on Table 3 show that only spectral Band 4-Red meets the requirements to be developed into a water turbidity mapping and monitoring algorithm because the P-value = 0.002089 is smaller than α = 0.05. Band 2-Blue, Band 3-Green and Band 8-NIR cannot be analysed further because the P-value does not have a significant effect as the value is greater than α = 0.05.

The turbidity mapping and monitoring algorithm used in this study is based on the Regression Statistics test using a single band from the Sentinel 2B Satellite platform, namely Band 4-Red with a spectral value of 665 nm. The regression test results obtained the equation of the digital value of Band 4-Red with in situ turbidity data found the equation:

$$y = ((0.012x) - 1.8323);$$

where y is the in situ turbidity value, x is the digital value of the Sentinel 2B image of the Band 2-red channel.

Furthermore, the spatial transformation process of the equation found an algorithm for water turbidity that can be used for the function of mapping and monitoring turbidity in seagrass habitats (Figure 6) with the algorithm formula:

$$TU = ((0.012 * Rrs665) - 1.8323) - \varrho;$$

where TU is the turbidity value (NTU), Rrs665 is Band 2-red (nm), and ϱ is the correction factor for turbidity values at image pixels equal to 0.

The new image applying the algorithm results in this study (Figure 6) used a correction factor of ϱ = 0.25. This correction value is found from the average variance of the spectral values resulting from the algorithm, which is constructed from a liner regression equation between the digital Band 4-Red values and the in situ data. The value of this correction factor ϱ can differ because it depends on the quality of the image used and the characteristics of the ocean waters.

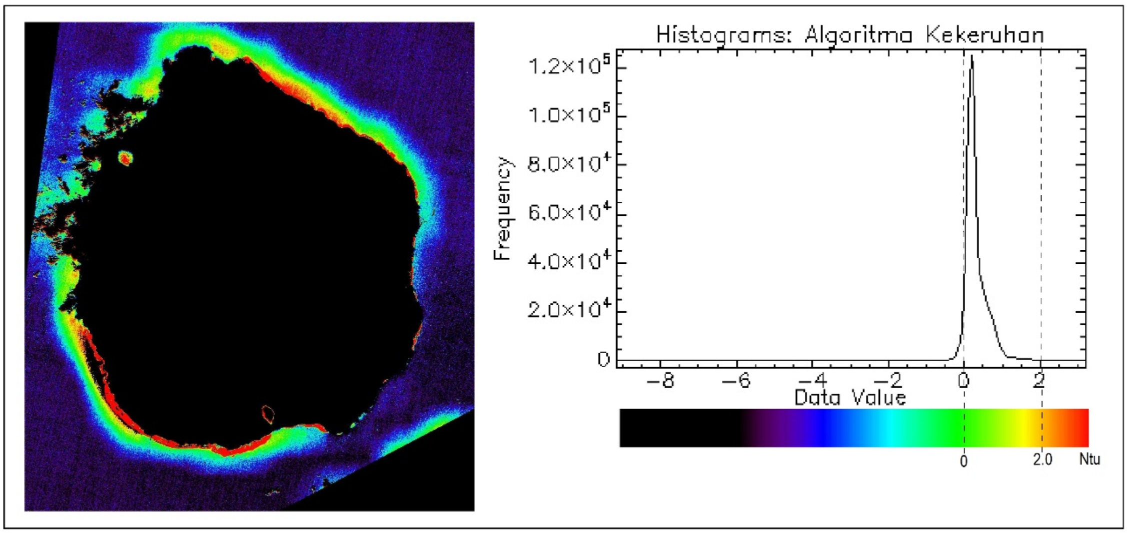

Figur 6. Results of new image algorithm for mapping and monitoring water turbidity (NTU)

Algorithm validation results for water turbidity

The water turbidity algorithm between Katlane *et al.*, (2020) and the new algorithm found was validated statistically using Normalized Mean Absolute Error (NMAE) and the coefficient of determination (R^2). Validation of the algorithm model in this research is carried out to determine the level of accuracy of each model application. Based on Table 4, the NMAE value of the Katlane *et al.* (2020) algorithm is 50.44% and the new turbidity algorithm found has a value of 29.38%. This result shows that the NMAE value of the Katlane *et al.*, (2020) algorithm is greater than the NMAE value of the new turbidity algorithm found.

Table 4. Validation of the two turbidity algorithm models based on NMAE value in Ternate Island.

Sampling Points	In situ Data	Algoritma Katlane et al (2020)	New Turbidity Algorithm	Difference between Measurement Data and Model Data	
	(a)	(b)	©	(la-bl)	(la-cl)
K1	1.5	1.982	1.384	0.482	0.116
K2	1.4	1.917	1.319	0.517	0.081
K3	1.4	1.871	1.274	0.471	0.126
J1	1.1	1.832	1.235	0.732	0.135
J2	0.9	1.789	1.191	0.889	0.291
J3	1.2	1.883	1.285	0.683	0.085
P1	0.3	1.546	0.948	1.246	0.648

Sampling Points	In situ Data	Algoritma Katlane et al (2020)	New Turbidity Algorithm	Difference between Measurement Data and Model Data	
P2	0.7	1.732	1.134	1.032	0.434
P3	0.7	1.709	1.111	1.009	0.411
N1	0.6	1.718	1.12	1.118	0.52
N2	0.3	1.604	1.006	1.304	0.706
N3	0.3	1.403	0.805	1.103	0.505
Total	10.4	20.986	13.812	10.586	4.058
Average	0.866	1.748	1.151	0.882	0.338
NMAE	-	50.44 %	29.38 %	-	-

The results of the turbidity algorithm model validation based on the coefficient of determination (R^2) value of the water turbidity algorithm between the Katlane *et al.* (2020) algorithm and the new algorithm found obtained R^2 values that are not significantly different (Figure 7). The R^2 value of the Katlane *et al.* (2020) algorithm is 0.8822 and the new algorithm found with R^2 0.8827. The R^2 value proves that the new algorithm found in this study is still superior to the new algorithm.

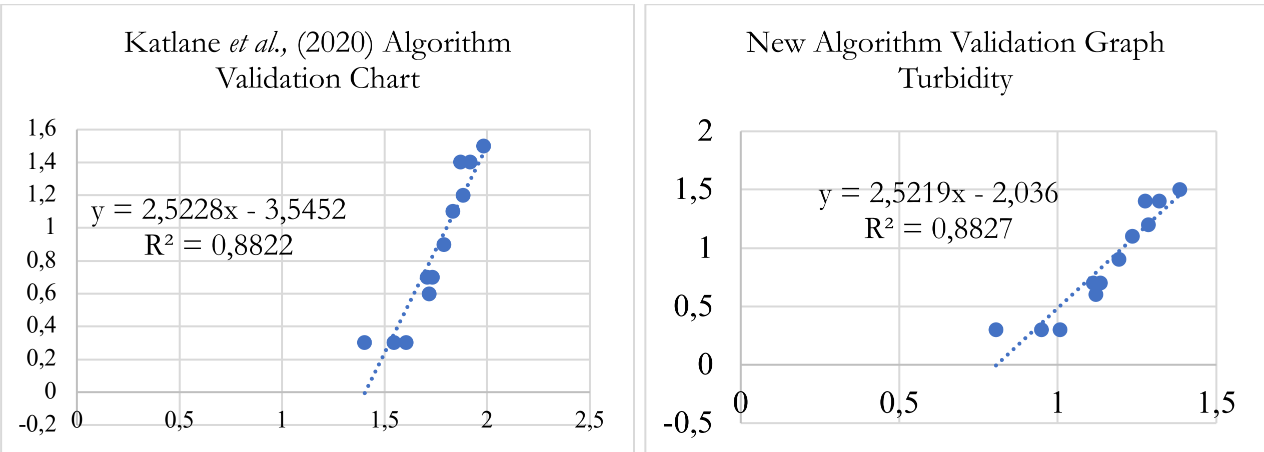

Figure 7. The coefficient of determination (R^2) of the water turbidity algorithm between the Katlane *et al.*, 2020 algorithm and the new algorithm

Discussion

The turbidity condition of seagrass habitat in each sampling location of Ternate Island obtained different values (Figure 2). Higher turbidity values were found in six sampling points, namely K1, K2, K3, J1, J2 and J3. The locations of these six sampling points are located in the southern part of Ternate Island which is geographically facing the Maluku Sea. Wave dynamics generated by winds from the Moluccas Sea can reach seagrass areas during high tide conditions and cause turbidity from substrate stirring. Field observations showed that the sediment composition around the seagrass habitat was muddy sand. In addition, the turbidity of the waters in this location is caused by the input of sediment from the mainland through a small river. The lower turbidity value of seagrass habitat on Ternate Island was found at six sampling points, namely P1, P2, P3, N1, N2 and N3. These six sampling points are coastal areas protected by Tidore Island so that the influence of waves coming from the Maluku Sea is relatively lower. Field observations found that the sediment composition around the sampling area is fine sand. Potential turbidity of waters in this location can be sourced from land that is dense with settlements and high human activity. Turbidity of coastal waters can be caused by unstable substrate types, turbidity inputs originating from land and human activities that cause sedimentation (Petus *et al.*, 2014; Baihaqi, 2019; Irawan, 2017; Mooselu *et al.*, 2024). Based on the Seawater Quality Standards, the turbidity quality of seagrass habitat waters is still good because it is less than 5 NTU (Decree of the Minister of Environment Number: 51 of 2004). Seagrasses can develop well if the water conditions are in a clear state, namely water turbidity is less than 3 NTU (Bulmer *et al.,* 2018; Troxell *et al.,* 2024; Kenyon *et al.,* 2024).

The results of in situ turbidity data measurements obtained were used as validation for the development of the Sentinel 2B image data algorithm model used in this study. The Sentinel 2B image data used in this study is subjected to a data recovery process from several errors aimed at minimizing the bias value so as to increase the image accuracy value. The image quality recovery steps include geometric, atmospheric, radiometric, land masking, and sun glint corrections. Geometric and atmospheric correction of Sentinel 2B imagery is done automatically using the Sen2Cor Processor plugin found in SNAP Software based on the included meta data file so that the data error level is adjusted to the standard error tolerance. Radiometric digital value correction is a corrective step to restore the true digital value of image reflectance to improve the accuracy and quality of the data before it is used in further analysis. Image acquisition enhancement through land masking is a processing process that is also very important in marine environmental studies.

Land masking in image processing serves to eliminate land pixels so that it focuses more on analyzing waters (Mikelsons *et al.*, 2021; Mather. 2004; Paembonan *et al.,* 2018). Other benefits of image landmasking are reducing image data noise so that the analyzed image is the target image of the water, faster data processing because computation is only carried out within the scope of the research area, and increasing classification accuracy. The Sentinel 2B image used in this research is disturbed by the reflection of sunlight on the sea surface detected by the sensor. Sun glint correction is a very important image quality restoration process. Sun glint correction in this study was performed on Band 2-Blue, Band 3-Green, and Band 4-Red with an empirical approach using NIR correction (Hedley *et al.,* 2005; Harmel *et al.,* 2018) (Figure 4).

Mapping and monitoring of water turbidity of seagrass habitat in Ternate Island applying the algorithm model developed by Katlane *et al.,* (2020). The image data used is Sentinel 2B Band 4-Red image. The modeling results obtained can describe the spatial distribution of turbidity horizontally with higher turbidity values around the coast which is a seagrass habitat (Figure 5). The results of the regression analysis between the digital value of the modeling results and the in situ data obtained a coefficient of determination (R^2) of 0.8822. This R^2 value illustrates that the consistency of the tested digital values with the actual data has a significant relationship so that the modeling algorithm is scientifically acceptable.

The development of a new algorithm model using the Sentinel 2B platform for mapping and monitoring the turbidity of seagrass habitat waters in Ternate Island obtained good results (Figure 6). The new turbidity algorithm model created in this study provides a good distribution of turbidity in the waters of Ternate Island. The algorithm model is derived from regression analysis between Band 4-Red (Rrs665) and in situ data. The coefficient of determination (R^2) value obtained from the results of this modeling shows a significant relationship of 0.8827. Based on the R^2 value, the new turbidity algorithm model found in this study provides a good and accurate picture of the distribution of turbidity in Ternate Island.

Mapping and validation research of spatial algorithm for monitoring turbidity of seagrass habitat waters using Sentinel-2B imagery in Ternate Island using two turbidity algorithm models. The algorithm in this study uses the Katlane *et al.* (2020) algorithm and a new turbidity algorithm. Both algorithms used are estimation models so that validation tests need to be carried out.

Table 5. The validation results of the algorithm model used in this research

Type of turbidity algorithm	Model Equation	NMAE Value	R^2 Value	Platform
Algorithm Katlane *et al.,* (2020)	$TU = \frac{(Rrs665-0.014)}{0.013}$	50.44	0,8822	Sentinel 2B
New turbidity algorithm	TU = ((0.012* $Rrs665$)-1.8323)- ϱ	29.38	0,8827	Sentinel 2B

The Katlane *et al.* (2020) turbidity algorithm modeling and the new algorithm created in the study were validated using Normalized Mean Absolute Error (NMAE) and the coefficient of determination

(R^2). In Table 5, it is known that the mapping and monitoring of turbidity of seagrass habitat waters on Ternate Island with the application of the new algorithm is better than the Katlane *et al.,* (2020) algorithm. The application of the new algorithm obtained an NMAE value of 29.38 while Katlane *et al.,* (2020) obtained an NMAE value of 50.44. Statistically, the smaller NMAE value is an indicator that the model used is closer to the true value. The R2 value of the two models obtained almost the same value. The Katlane *et al.,* (2020) algorithm model in this study can be interpreted as 88.22% of the variability of the turbidity insitu data as dependent has been explained by the algorithm model as an independent variable. The interpretation of the new algorithm model is slightly superior with an R^2 value of 88.27%.

Conclusion

Turbidity of seagrass habitat waters in Ternate Island based on in situ data still meets seawater quality standards with turbidity values ranging from 0.3 NTU to 1.5 NTU. The application of remote sensing algorithms using the Katlane *et al.* (2020) algorithm model and the development of new algorithms can estimate the distribution of water turbidity with values that are not significantly different from the in situ data. The new turbidity algorithm model created in this study is more accurate than the Katlane *et al.* (2020) algorithm model based on the validation results obtained using Normalized Mean Absolute Error (NMAE) and a better coefficient of determination (R^2) value.

Acknowledgment

The authors extend their gratitude to The Indonesian Education Scholarship (Beasiswa Pendidikan Indonesia), Center for Higher Education Funding and Assessment from Ministry of Higher Education, Science, and Technology of Republic Indonesia, Endowment Fund for Education Agency (LPDP), Ministry of Finance of Republic Indonesia and to research collaborators for their invaluable contributions. (BPI Scholarship with ID Number: 202209091950)

References

Banh, Q.Q.T., J.L. Guppy, J.A. Domingos, A.M. Budd, R.C.C. Pinto, A.F. Marc, D.R. Jerry. 2021. Induction of precocious females in the protandrous barramundi (Lates calcarifer) through implants containing 17β-estradiol - effects on gonadal morphology, gene expression and DNA methylation of key sex genes. Aquaculture 539:736601. doi:https://doi.org/10.1016/j.aquaculture.2021.736601

Al Tanto, T, Nia Naelul HR, I. Ilham. 2018. Kualitas Air Laut Untuk Mendukung Wisata Bahari Dan Kehidupan Biota Laut (Studi Kasus: Sekitar Kapal Tenggelam Sophie Rickmers, Perairan Prialaot Sabang). Jurnal Kelautan. 11(2):173-183. DOI: https://doi.org/10.21107/jk.v11i2.4276

Ajiperwata, D., E. Indrayanti, B. Rochaddi. 2023. Sebaran Material Padatan Tersuspensi Berdasarkan Data Citra Sentinel-2 di Perairan Tanjung Jati, Jepara. Jurnal Kelautan Tropis, Vol. 26(2):349-356. doi:10.14710/jkt.v26i2.18468.

Bulmer, R.H., M. Townsend, T. Drylie, A.M. Lohrer. 2018. Elevated turbidity and the nutrient removal capacity of seagrass. Frontiers in Marine Science, 5:462. https://doi.org/10.3389/fmars.2018.00462

Baihaqi, R. 2019. Konservasi Jenis Lamun di Kawasan Perairan Pulau Pramuka, Kepulauan Seribu, Provinsi DKI Jakarta. Jurnal Geografi Gea, 19(1):42-47. https://doi.org/10.17509/gea.v19i1.14780.g9942

Cahyaningsih, D.P., H. Hartono. 2018. Pemetaan Habitat Bentik dengan Citra Multispektral Sentinel-2A di Perairan Pulau Menjangan Kecil dan Menjangan Besar, Kepulauan Karimunjawa. Jurnal Bumi Indonesia 7(3). https://www.neliti.com/publications/260747/pemetaan-habitat-bentik-dengan-citra-multispektral-sentinel-2a-di-perairan-pulau#cite

Chisholm, W. J. 2009. The stability of shallow coastal sediments with and without seagrasses [Murdoch University]. https://researchportal.murdoch.edu.au/esploro/outputs/doctoral/The-stability-of-shallow-coastal-sediments/991005540010507891#file-0

Davies-Colley, R. J., D. G. Smith. 2007. Turbidity, Suspended Sediment, and Water Clarity: A Review. Journal of the American Water Resources Association, 37(5), 1085-1101. https://doi.org/10.1111/j.1752-1688.2001.tb03624.x

Dewi, C.S., B. Subhan, D. Arafat. 2017. Keragaman, kerapatan dan penutupan lamun di Pulau Biak, Papua. Depik Jurnal Ilmu-Ilmu Perairan, Pesisir dan Perikanan 6(2):122-127. DOI: https://doi.org/10.13170/depik.6.2.6227

Dewi, S.K., W. A. Setyati, I. Riniatsih. 2021. Stok Karbon pada Ekosistem Lamun di Pulau Kemujan dan Pulau Bengkoang Taman Nasional Karimunjawa. 10(1):39-47. Journal of Marine Research, vol. 10, no. 1, pp. 39-47, Feb. 2021. https://doi.org/10.14710/jmr.v10i1.28273

Duarte, C. M., S. Tomas, and Nuria Marba, 2013, Assessing the CO2 capture potential of seagrass restoration projects. Journal of Applied Ecology 2013, 50, 1341–1349. doi: 10.1111/1365-2664.12155

Harmel, T., M. Chami, T. Tormos, N. Reynaud, P. A. Danis. 2018. Sunglint correction of the Multi-Spectral Instrument (MSI)-SENTINEL-2 imagery over inland and sea waters from SWIR bands. Remote Sensing of Environment 204:308-321. doi:https://doi.org/10.1016/j.rse.2017.10.022

Hedley, J. D., A. R. Harborne, P. J. Mumby. 2005. Technical note: Simple and robust removal of sun glint for mapping shallow-water benthos. International Journal of Remote Sensing, 26(10), 2107–2112. doi:10.1080/01431160500034086

Irawan, A. 2017. Potensi cadangan dan serapan karbon oleh padang lamun di bagian utara dan timur Pulau Bintan. Oseanologi dan Limnologi di Indonesia, 2(3):35-48. https://d1wqtxts1xzle7.cloudfront.net/68049279

Jo, R. O., S. Minsas, A. A. Kushadiwijaya, N. Idiawati. 2023. Analisis Kondisi Lamun Enhalus acoroides di Perairan Desa Sutera Kecamatan Sukadana Kabupaten Kayong Utara. Jurnal Akuatiklestari, 6(Edisi Khusus Seminar Nasional Perikanan Tangkap IX): 108-115. DOI: https://doi.org/10.31629/akuatiklestari.v6i.5152

Katlane, R., C. Dupouy, B. El Kilani, J. C. Berges. 2020. Estimation of chlorophyll and turbidity using sentinel 2A and EO1 data in Kneiss Archipelago Gulf of Gabes, Tunisia. International Journal of Geosciences, 11:p. 708-728. https://doi.org/10.4236/ijg.2020.1110035

Kenyon, R.A., C. Y. Burridge, I. R. Poiner, R. C. Pendrey, M. L. Tonks. 2024. Impact of ship-way channel dredging on a seagrass community in the Gulf of Carpentaria, Australia. Ocean & Coastal

Management 249:107010. doi:https://doi.org/10.1016/j.ocecoaman.2023.107010

Lessy, M. R., Y. Ramili. 2018. Restorasi lamun; studi transplantasi lamun Enhalus acaroides di perairan pantai Kastela, Kota Ternate. Jurnal Ilmu Kelautan Kepulauan, 1 (1) ; 40 – 47. DOI: https://doi.org/10.33387/jikk.v1i1.680.

Mather, P.M. 2004, Computer Processing of Remotely-Sensed Images, An Introduction, 3rd ed., John Wiley & Sons Ltd., West Sussex.

Mikelsons, K., M. Wang, X-L. Wang, L. Jiang. 2021. Global land mask for satellite ocean color remote sensing. Remote Sensing of Environment 257:112356. doi:https://doi.org/10.1016/j.rse.2021.112356

Mooselu, M. G., M. R. Nikoo, H. Liltved, M. S. Bjørkenes, A. Elnashar, S. A. Shojaeezadeh, T. K. D. Weber. 2024. Assessing road construction effects on turbidity in adjacent water bodies using Sentinel-1 and Sentinel-2. Science of The Total Environment 957:177554. doi:https://doi.org/10.1016/j.scitotenv.2024.177554

Najamuddin, Inayah, R. Labenua, M. F. Samawi, K. Yaqin, R. E. Paembonan, F. Ismail, Z. A. Harahap. 2024. Distribution of heavy metals Hg, Pb, and Cr in the coastal waters of small islands of Ternate, Indonesia. Ecological Frontiers 44(3):529-537. doi:https://doi.org/10.1016/j.chnaes.2023.09.002.

Ondiviela B, I. J. Losada, J. L. Lara, M. Maza, C. Galván, T. J. Bouma, J. van Belzen. 2014. The role of seagrasses in coastal protection in a changing climate. Coastal Engineering 87:158-168. doi:https://doi.org/10.1016/j.coastaleng.2013.11.005

Paembonan, R. E., M. D. Achmad, I. Marus, S. Baddu, A. Karman, Najamuddin, N. Akbar, N. M. N. Natih, I. Tahir, E. S. Wibowo, D. Muksin, Neviaty P Zamani, F. Ismail. 2022. Hutan mangrove di Pulau Ternate secara spasial dan temporal. Jurnal Ilmu Kelautan Kepulauan, 5 (2); 656-667. DOI: https://doi.org/10.33387/jikk.v5i2.5687

Paembonan, R. E., M. A. Amran, F. Ismail. 2018. Perhitungan nilai digital radiansi berdasarkan band pada citra alos avnir-2 di wilayah sidangoli dehe kecamatan jailolo selatan kabupaten halmahera barat. Jurnal Ilmu Kelautan Kepulauan 1(2). DOI: https://doi.org/10.33387/jikk.v1i2.940

Petus, C., C. Collier, M. Devlin, M. Rasheed and S. McKenna. 2014. Using MODIS data for understanding changes in seagrass meadow health: A case study in the Great Barrier Reef (Australia). Marine Environmental Research 98: 68-85. https://doi.org/10.1016/j.marenvres.2014.03.006

Rahmad, R., M. Masita, N. Riyadi. 2019. Penggunaan Data Citra Satelit Sentinel 2A Guna Mendukung Pemilihan Pantai Pendaratan Amphibi (Studi Kasus Pulau Selaru): Use of Sentinel 2A Satellite Imagery Data to Support Amphibious Landing Beach Selection (Selaru Island Case Study). Jurnal Chart Datum, 5(2):155-168. https://doi.org/10.37875/chartdatum.v5i2.153

Sari, S. N., E. Nurfaizi, Y. Anjeli, A. J. Topano. 2021. Peranan Penting Ekosistem Padang Lamun (Seagrass) Dalam Penunjang Kehidupan Dan Perkembangan Biota Laut. GHAITSA: Islamic Education Journa 2(3). doi: https://doi.org/10.62159/ghaitsa.v2i2.847

Sarinawaty, P., F. Idris F, A. H. Nugraha. 2020. Karakteristik morfometrik lamun Enhalus acoroides dan Thalassia hemprichii di Pesisir Pulau Bintan. Journal of Marine Research 9(4):474-484. https://doi.org/10.14710/jmr.v9i4.28432

Supriyadi, I. H., H. A. Cappenberg, J. Souhuka, P. C. Makatipu, M. Hafizt. 2018. Kondisi Terumbu Karang, Lamun Dan Mangrove Di Suaka Alam Perairan Kabupaten Raja Ampat Provinsi Papua Barat. Jurnal Penelitian Perikanan Indonesia 23(4):241-252. doi:http://dx.doi.org/10.15578/jppi.23.4.2017.241-252

Troxell, K., B. Schonhoff, M. Kershaw, M. Ceccopieri, T. Crowl, P. Gardinali. 2024. Near real-time monitoring of the Biscayne Bay Watershed (South Florida, USA) and major tributaries by water quality research buoys. Science of The Total Environment 955:177203. doi:https://doi.org/10.1016/j.scitotenv.2024.177203

Wicaksono, P., M. A. Fauzan, I. S. W. Kumara, R. N. Yogyantoro, W. Lazuardi, Z. Zhafarina. 2019. Analysis of reflectance spectra of tropical seagrass species and their value for mapping using multispectral satellite images. International Journal of Remote Sensing 40(23):8955-8978. https://doi.org/10.1080/01431161.2019.1624866

Xu, M., B. B. Barnes, C. Hu, P. R. Carlson, L. A. Yarbro. 2023. Water clarity monitoring in complex coastal environments: Leveraging seagrass light requirement toward more functional satellite ocean color algorithms. Remote Sensing of Environment 286:113418. doi:https://doi.org/10.1016/j.rse.2022.113418

How to cite this paper:

Paembonan, R. E., D. G. Bengen, I. W. Nurjaya, S. B. Agus, N. M. N. Natih, B. Subhan, J. Santoso. 2025. Mapping and validation of spatial algorithm for monitoring turbidity of seagrass habitat using Sentinel-2B imagery in Ternate Island. Depik Jurnal Ilmu-Ilmu Perairan, Pesisir dan Perikanan, Special Issue The 5th ICFM: 75–86.